Supporting Information

Cyclic Pt_3Ag_{33} and $Pt_3Au_{12}Ag_{21}$ Nanoclusters with the M_{13} Icosahedra as Building-blocks

Sha Yang, Jinsong Chai, Ying Lv, Tao Chen, Shuxin Wang, Haizhu Yu* and Manzhou Zhu*

Department of Chemistry and Centre for Atomic Engineering of Advanced Materials, Anhui Province Key Laboratory of Chemistry for Inorganic/Organic Hybrid Functionalized Materials, Anhui University, Hefei, Anhui, 230601, China.

1. Materials.

All reagents and solvents were commercially available and use without further purification. The tetrachloroauric(III) acid ($HAuCl_4•4H_2O$, ≥99.99% metals basis) was purchased from the China Nonferrous Metal Mining (Group) Co., Ltd. (Shenyang, China). The silver p-toluenesulfonate ($C_7H_7AgO_3S$, ≥98%, metal basis), chloroplatinic acid hexahydrate ($H_2PtCl_6•6H_2O$, ≥99.99%, metal basis), triphenylphosphine (Ph_3P, ≥ 99%) and sodium borohydride ($NaBH_4$, ≥ 98%) were received from Aldrich (Shanghai, China). All solvents in the experiment are chromatographically pure and were purchased from Aldrich (Shanghai, China). Pure water was purchased from Wahaha Co. Ltd. All glassware was thoroughly cleaned with aqua regia (HCl: HNO_3 = 3:1, v:v), rinsed with copious pure water, and then dried in an oven prior to use.

2. Synthesis of Pt_3Ag_{33} nanocluster.

The synthesis of the bimetallic $[Pt_3Ag_{33}(PPh_3)_{12}Cl_8]^+$ nanocluster includes two steps. First, 58 mg silver *p*-toluenesulfonate (0.2 mmol) was mixed with 167 mg PPh_3 (0.64 mmol) and dissolved in 12 mL ethanol. The solution was stirred for 10 mins. Then, 20 mg $NaBH_4$ (0.5 mmol, dissolved in the 3 mL ethanol was added to the above solution. The second step is the addition of H_2PtCl_6. An amount of 51.8 mg $H_2PtCl_6•6H_2O$ (0.1 mmol, dissolved in the 50 uL pure water) was added to the above solution and then the solution was continued to be stirred for 16 hours. The product was collected by centrifugation (Pt_3Ag_{33} nanoclusters are insoluble in ethanol).

3. Synthesis of $Pt_3Au_{12}Ag_{21}$ nanocluster.

20 mg of $[Pt_3Ag_{33}(PPh_3)_{12}Cl_8]^+$ nanoclusters was dissolved in 5 mL CH_2Cl_2, and then 5 mg $Au(PPh_3)Cl$ complex was added. The solution was stirred for 5 seconds and the dichloromethane solution containing the $Pt_3Au_{12}Ag_{21}$ nanocluster was evaporated to dryness.

4. X-ray crystallographic determination of Pt_3Ag_{33} and $Pt_3Au_{12}Ag_{21}$ nanoclusters.

The diffraction data of the single crystals were collected on Bruker APEX-II CCD diffractometer using Mo Kα radiation (λ= 0.71073 Å). The crystal structures were determined by direct methods and refined by using the full-matrix least-squares methods within the XL (Sheldrick, 2008) and the ShelXT program (Sheldrick, 2015) for Pt_3Ag_{33} and $Pt_3Au_{12}Ag_{21}$ nanoclusters, respectively. The placement of the heteroatoms and fractional site occupancy in these alloy nanoclusters were ascertained by the method of modifying the disorderly free variables.

5. Computational method and details.

Density function theory (DFT) and Time-dependent Density function theory (TDDFT) calculations were implemented by ADF software.[1] For reducing the computational cost, 2,4-dimethylthiophenol and triphenylphosphine ligands were simplified with SCH_3 and PMe_3 in calculations. The geometry optimizations of clusters were calculated using GGA: PBE functional[2,3] with scalar relativistic and a triple-ζ polarized (TZP) basis set. The frozen core approximation was applied to core electrons. Based on the optimized structure of clusters, UV-vis spectra were calculated at GGA: BP/TZP levelith Spin-Orbit relativistic.[4]

6. Characterization.

Ultraviolet-visible (UV-vis) absorption spectra were recorded on an Agilent 8453 spectrophotometer with CH_2Cl_2 as the solvent. X-ray photoelectron spectroscopy (XPS) measurements were performed on a thermal ESCALAB 250, equipped with a monochromated Al Kα (1486.8 eV) 150 W X-ray source, 0.5 mm circular spot size, and a flood gun (to counter charging effects). The analysis chamber base pressure was lower than 1×10^{-9} mbar, and data was collected with FAT = 20 eV. Electrospray ionization time-of-flight mass spectrometry (ESI-TOF-MS) measurement was performed by a Micr OTOF-QIII high-resolution mass spectrometer. The source temperature maintained at 80 ^{o}C. The sample was directly infused into the chamber at 5 μL/min. ESI samples were prepared by dissolving the clusters in dichloromethane (0.1 mg/mL). Thermal gravimetric analysis (TGA) was conducted on samples of about 10 mg, under an atmosphere of anhydrous N_2 (flow rate 50 mL/min), using a TG/DTA 6300 analyzer (Seiko Instruments, Inc), with a heating rate of 10 ^{o}C/min. Nuclear magnetic resonance (NMR) analysis was performed on a Bruker AM spectrometer operating at 400 MHz for ^{1}H; CD_2Cl_2 was used as the solvent to dissolve 25 mg clusters. Photoluminescence (PL) spectra were measured on a FL-4500 spectrofluorometer with the same optical density (OD) ~0.05. In these experiments, the nanoclusters solution was prepared in CH_2Cl_2 at a concentration of less than 1 mg mL^{-1}.

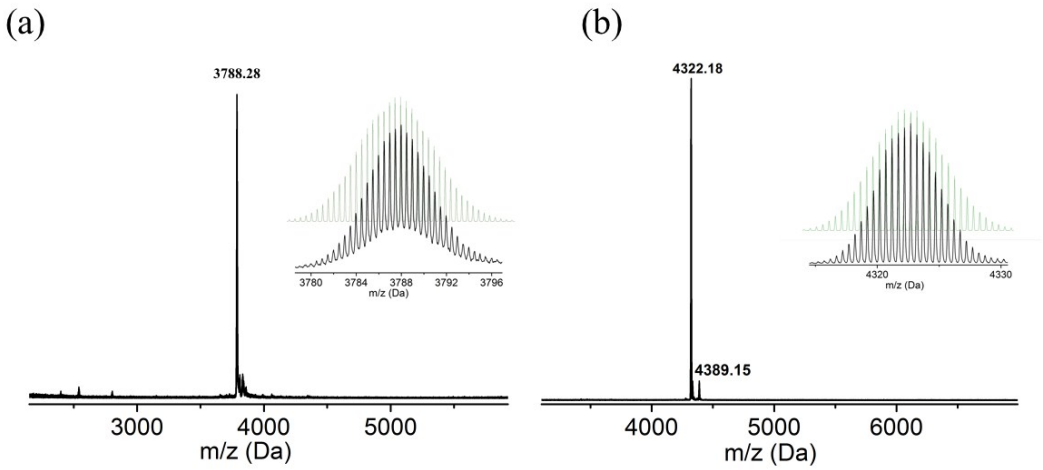

Figure S1. The ESI-MS spectrum of the $[Pt_3Ag_{33}(PPh_3)_{12}Cl_8]^+$ nanocluster (a) and $[Pt_3Ag_{21}Au_{12}(PPh_3)_{12}Cl_8]^+$ nanocluster (b). Inset: The measured (black trace) and simulated (green trace) isotopic patterns of $Pt_3Ag_{33}(PPh_3)_{12}Cl_8+H]^{2+}$ nanocluster (a) and $[Pt_3Ag_{21}Au_{12}(PPh_3)_{12}Cl_8+H]^{2+}$ nanocluster (b), respectively.

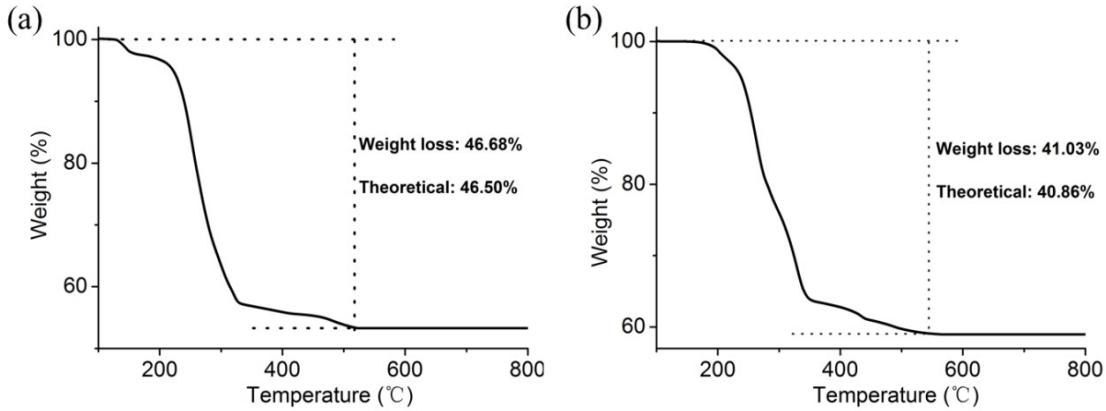

Figure S2. The TGA curve of the $[Pt_3Ag_{33}(PPh_3)_{12}Cl_8]^+$ nanocluster (a) and $[Pt_3Ag_{21}Au_{12}(PPh_3)_{12}Cl_8]^+$ nanocluster (b).

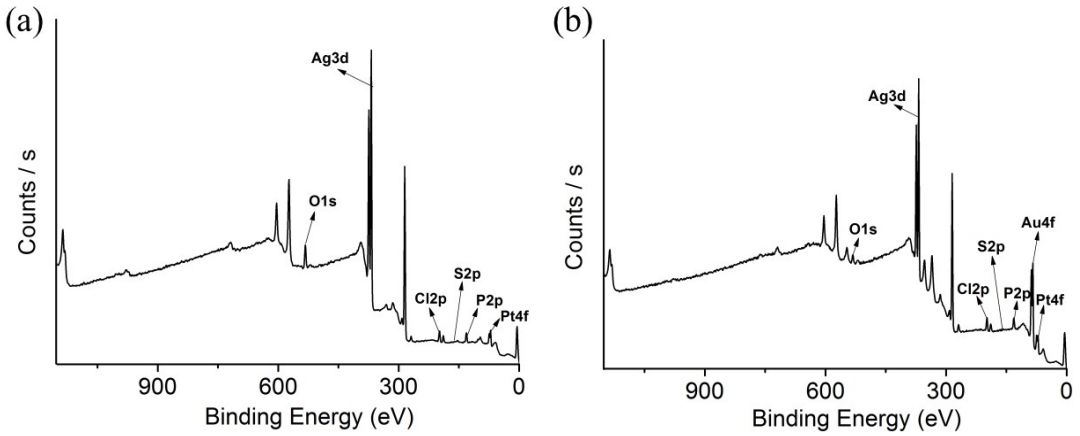

Figure S3. The full XPS spectrum of the $[Pt_3Ag_{33}(PPh_3)_{12}Cl_8]^+$ nanocluster (a) and $[Pt_3Ag_{21}Au_{12}(PPh_3)_{12}Cl_8]^+$ nanocluster (b).

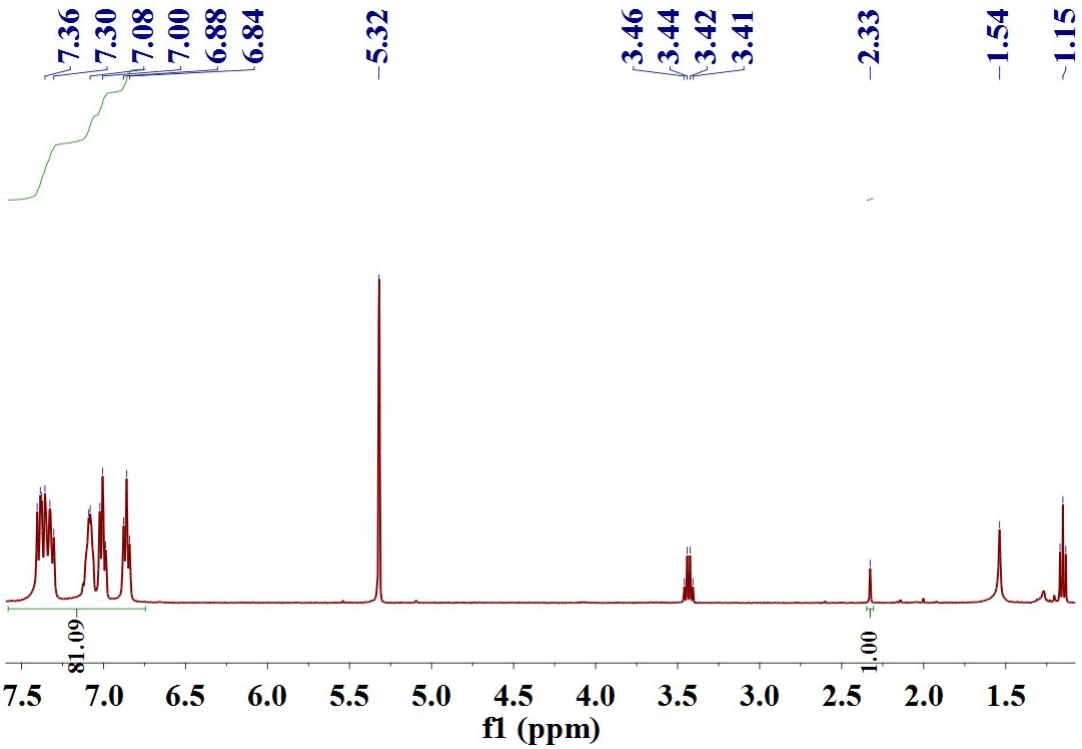

Figure S4. The ^1H NMR spectrum of the $[Pt_3Ag_{33}(PPh_3)_{12}Cl_8]^+$ nanocluster (δ (2.33) is assigned to $-CH_3$ of p-toluenesulfonate, δ (1.54) is assigned to H_2O, δ (3.44) and δ (1.15) are assigned to $CH_3CH_2OCH_2CH_3$).

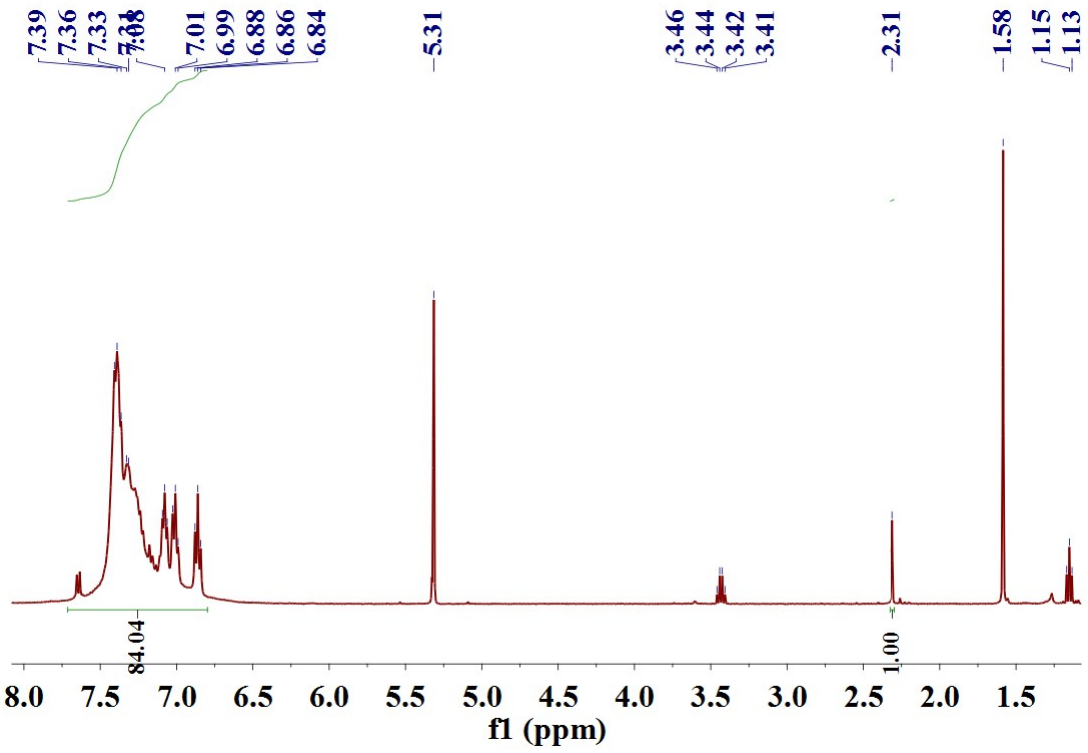

Figure S5. The ^{1}H NMR spectrum of the $[Pt_3Ag_{21}Au_{12}(PPh_3)_{12}Cl_8]^+$ nanocluster (δ (2.31) is assigned to $–CH_3$ of p-toluenesulfonate, δ (1.58) is assigned to H_2O, δ (3.44) and δ (1.15) are assigned to $CH_3CH_2OCH_2CH_3$).

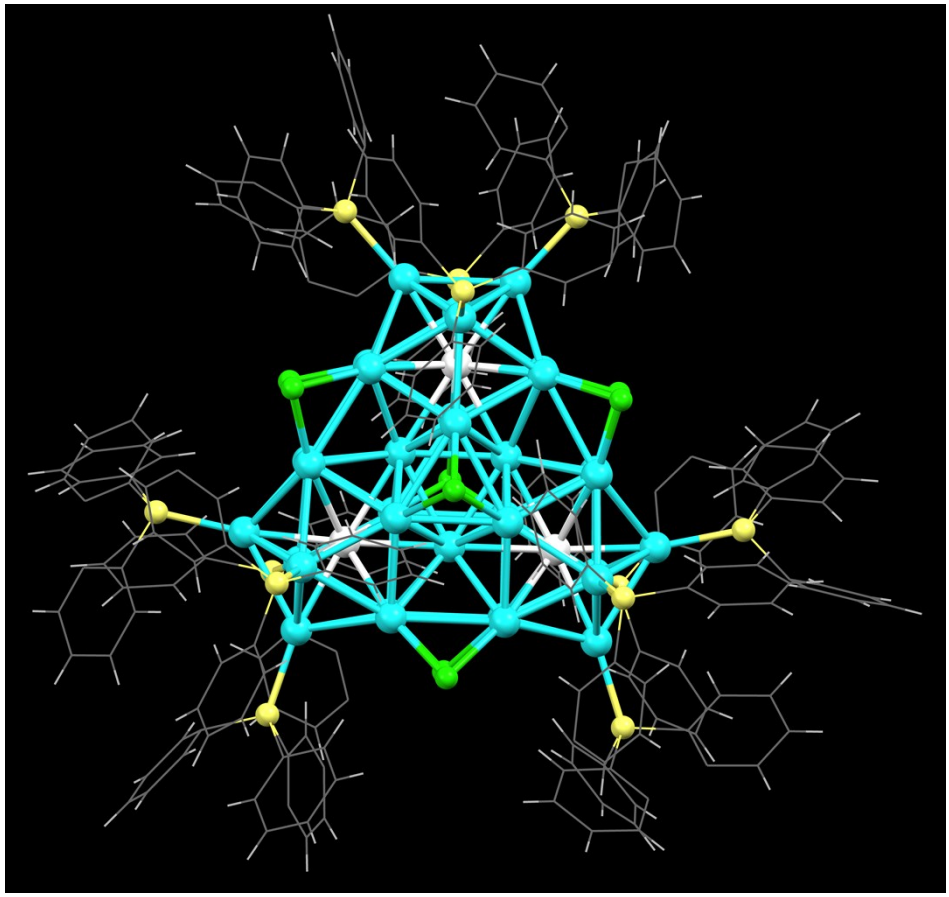

Figure S6. The total structure of the $[Pt_3Ag_{33}(PPh_3)_{12}Cl_8]^+$ NC (color labels: cyan = Ag; white = Pt; green = Cl; yellow = P; gray = C; and white = H).

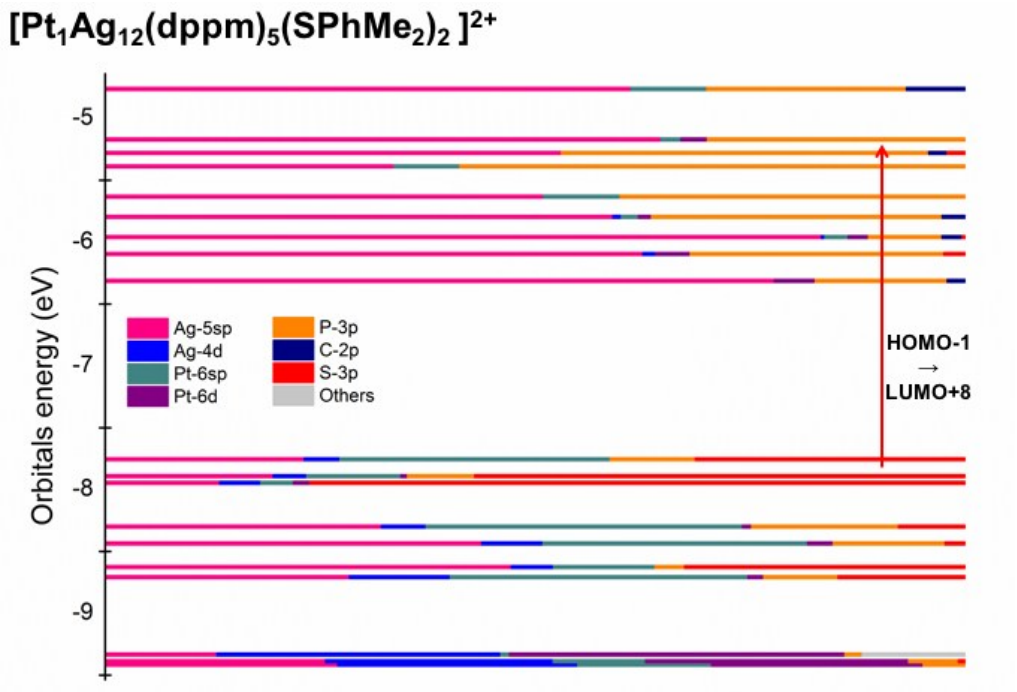

Figure S7. The Kohn–Sham orbital energy level diagram for of the $[Pt_1Ag_{12}(dppm)_5(SPhMe_2)_2]^{2+}$ nanocluster.

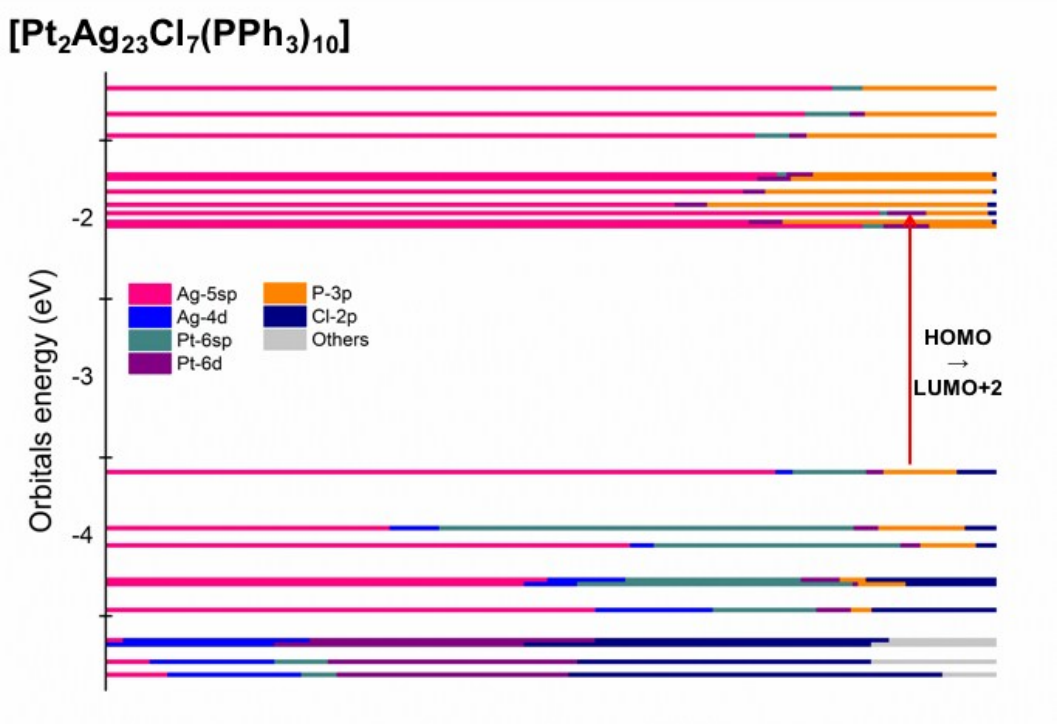

Figure S8. The Kohn–Sham orbital energy level diagram for of the $[Pt_2Ag_{23}(PPh_3)_{10}Cl_7]$ nanocluster.

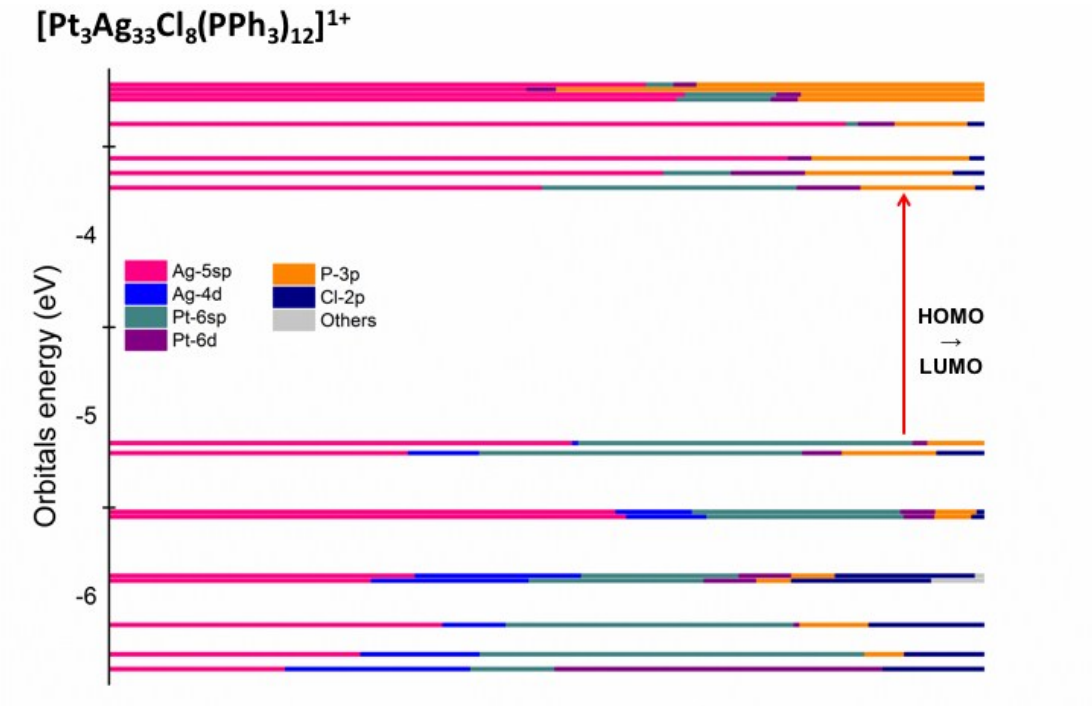

Figure S9. The Kohn–Sham orbital energy level diagram for of the $[Pt_3Ag_{33}(PPh_3)_{12}Cl_8]^+$ nanocluster.

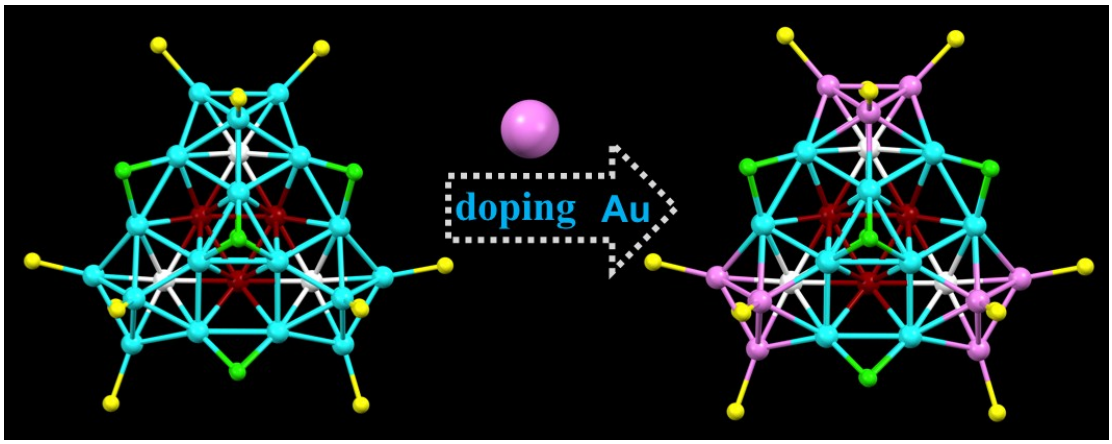

Figure S10. The core structure of the $[Pt_3Au_{12}Ag_{21}(PPh_3)_{12}Cl_8]^+$ NC. (color labels: cyan/dark red = Ag; white = Pt; magenta=Au; green = Cl; yellow =P; all C and H atoms are not shown).

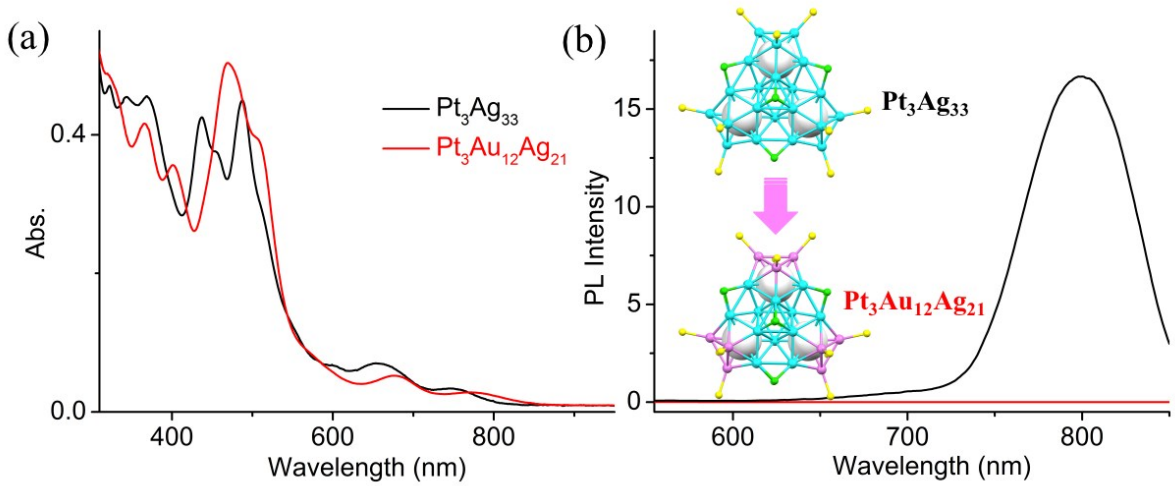

Figure S11. (a) UV-vis and (b) PL spectra of the Pt_3Ag_{33} (black line) and $Pt_3Au_{12}Ag_{21}$ (red line) nanoclusters (color labels: cyan = Ag; white = Pt; magenta=Au; green = Cl; yellow =P; all C and H atoms are not shown)

Table S1. The bond lengths distribution in the $[Pt_3Ag_{33}(PPh_3)_{12}Cl_8]^+$ nanocluster (color labels: cyan = Ag; white = Pt; green = Cl; yellow =P; all C and H atoms are not shown).

Bond	**Ag-P**	**Ag-Cl**		**Ag-Ag**		**Ag-Pt**
Site	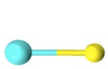	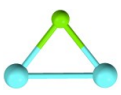		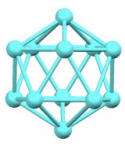	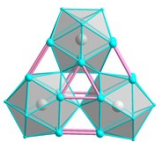	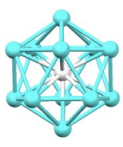

Range (Å)	2.394-2.421	2.478-2.488	2.535-2.546	2.846-2.995	3.010-3.063	2.681-2.837
Average (Å)	**2.412**	**2.481**	**2.540**	**2.889**	**3.037**	**2.749**

Table S2. Crystal data and structure refinement for the $[Pt_3Ag_{33}(PPh_3)_{12}Cl_8]^+$ nanocluster.

Identification code	$Pt_3Ag_{33}(PPh_3)_{12}Cl_8$
Empirical formula	$C_{216}H_{180}Pt_3Ag_{33}Cl_8P_{12}$
Formula weight	7575.89 g/mol
Temperature	296(2) K
Wavelength	0.71073 Å
Crystal system	trigonal
Space group	P -3
Unit cell dimensions	a=23.942(2) Å α=90°
	b=23.942(2) Å β=90°
	c=25.622(2) Å γ=120°
Volume	12719(2) $Å^3$
Z	1.99998
Density (calculated)	1.978Mg/m^3
Absorption coefficient	4.315 mm^{-1}
F(000)	7154
Crystal size	0.15 x 0.1 x 0.05 mm^3
Theta range for data collection	2.528 to 27.48°
Index ranges	-29<=h<=29
	-29<=k<=29
	-31<=l<=31

Reflections collected	12823
Independent reflections	16540 [R(int) = 0.1672]
Completeness to theta = 25.24°	99.99%
Absorption correction	Multi scan
Data / restraints / parameters	16540 / 901 / 674
Goodness-of-fit on F^2	1.051
Final R indices [I>2sigma(I)]	R1=0.1396, wR2=0.2836
R indices (all data)	R1=0.1672, wR2=0.3060
Largest diff. peak and hole	3.138 and -4.102 e.$Å^{-3}$

Table S3. Crystal Data and Structure Refinement for the $[Pt_3Au_{12}Ag_{21}(PPh_3)_{12}Cl_8]^+$ nanocluster.

Identification code	$Pt_3Au_{12}Ag_{21}(PPh_3)_{12}Cl_8$	
Empirical formula	$C_{216}H_{180}Pt_3Au_{12}Ag_{33}Cl_8P_{12}$	
Formula weight	5844.10 g/mol	
Temperature	293(2) K	
Wavelength	0.71073 Å	
Crystal system	triclinic	
Space group	P -1	
Unit cell dimensions	a=20.78(3) Å	α=90.36(2)°
	b=22.54(4) Å	β=102.17(2)°
	c=27.60(4) Å	γ=92.03(2)120°
Volume	12682(34) $Å^3$	
Z	2	
Density (calculated)	1.537Mg/m^3	
Absorption coefficient	10.28 mm^{-1}	
F(000)	4949	
Theta range for data collection	2.15 to 24.67°	
Index ranges	-23<=h<=24	
	-26<=k<=26	
	-32<=l<=32	
Reflections collected	9658	
Independent reflections	41514 [R(int) = 0.3894]	
Completeness to theta = 25.24°	100%	
Data / restraints / parameters	41514 / 3 / 469	
Goodness-of-fit on F^2	1.040	
Final R indices [I>2sigma(I)]	R1=0.2464, wR2=0.5130	
R indices (all data)	R1=0.3894, wR2=0.5554	
Largest diff. peak and hole	7.553 and -4.241 e.$Å^{-3}$	

References

1. G. Velde, F. M. Bickelhaupt, E. J. Baerends, C. F. Guerra, S. J. A. Gisbergen, J. G. Snijders, T. Ziegler, Chemistry with ADF. *J. Comput. Chem.* **2001**, *22*, 931-967.

2. J. P. Perdew, K. Burke, M. Ernzerhof, Generalized Gradient Approximation Made Simple. *Phys. Rev. Lett.* **1996**, *77*, 3865-3868.

3. K. A. Kacprzak, L. Lehtovaara, J. Akola, O. Lopez-Acevedo and H. Häkkinen, A density functional investigation of thiolate-protected bimetal $PdAu_{24}(SR)_{18}^{z}$ clusters: doping the superatom complex. *Phys. Chem. Chem. Phys.* **2009**, 11, 7123-7129.

4. J. Autschbach, Perspective: Relativistic effects. *J. Chem. Phys.* **2012**, *136*, 150902.